EUROPEAN LABORATORY FOR PARTICLE PHYSICS

CERN-EP/99-084
21 June 1999

Search for Higgs Bosons and Other Massive States Decaying into Two Photons in e^+e^- Collisions at 189 GeV

The OPAL Collaboration

Abstract

A search is described for the generic process $e^+e^- \to XY$, where X is a neutral heavy scalar boson decaying into a pair of photons, and Y is a neutral heavy boson (scalar or vector) decaying into a fermion pair. The search is motivated mainly by the cases where either X, or both X and Y, are Higgs bosons. In particular, we investigate the case where X is the Standard Model Higgs boson and Y the Z^0 boson. Other models with enhanced Higgs boson decay couplings to photon pairs are also considered. The present search combines the data set collected by the OPAL collaboration at 189 GeV collider energy, having an integrated luminosity of 182.6 pb^{-1}, with data samples collected at lower energies. The search results have been used to put 95% confidence level bounds, as functions of the mass M_X, on the product of the cross-section and the relevant branching ratios, both in a model independent manner and for the particular models considered.

(Accepted by Physics Letters B)

The OPAL Collaboration

G. Abbiendi[2], K. Ackerstaff[8], G. Alexander[23], J. Allison[16], N. Altekamp[5], K.J. Anderson[9], S. Anderson[12], S. Arcelli[17], S. Asai[24], S.F. Ashby[1], D. Axen[29], G. Azuelos[18,a], A.H. Ball[8], E. Barberio[8], R.J. Barlow[16], J.R. Batley[5], S. Baumann[3], J. Bechtluft[14], T. Behnke[27], K.W. Bell[20], G. Bella[23], A. Bellerive[9], S. Bentvelsen[8], S. Bethke[14], S. Betts[15], O. Biebel[14], A. Biguzzi[5], I.J. Bloodworth[1], P. Bock[11], J. Böhme[14], D. Bonacorsi[2], M. Boutemeur[33], S. Braibant[8], P. Bright-Thomas[1], L. Brigliadori[2], R.M. Brown[20], H.J. Burckhart[8], P. Capiluppi[2], R.K. Carnegie[6], A.A. Carter[13], J.R. Carter[5], C.Y. Chang[17], D.G. Charlton[1,b], D. Chrisman[4], C. Ciocca[2], P.E.L. Clarke[15], E. Clay[15], I. Cohen[23], J.E. Conboy[15], O.C. Cooke[8], J. Couchman[15], C. Couyoumtzelis[13], R.L. Coxe[9], M. Cuffiani[2], S. Dado[22], G.M. Dallavalle[2], R. Davis[30], S. De Jong[12], A. de Roeck[8], P. Dervan[15], K. Desch[27], B. Dienes[32,h], M.S. Dixit[7], J. Dubbert[33], E. Duchovni[26], G. Duckeck[33], I.P. Duerdoth[16], P.G. Estabrooks[6], E. Etzion[23], F. Fabbri[2], A. Fanfani[2], M. Fanti[2], A.A. Faust[30], L. Feld[10], F. Fiedler[27], M. Fierro[2], I. Fleck[10], A. Frey[8], A. Fürtjes[8], D.I. Futyan[16], P. Gagnon[7], J.W. Gary[4], G. Gaycken[27], C. Geich-Gimbel[3], G. Giacomelli[2], P. Giacomelli[2], V. Gibson[5], W.R. Gibson[13], D.M. Gingrich[30,a], D. Glenzinski[9], J. Goldberg[22], W. Gorn[4], C. Grandi[2], K. Graham[28], E. Gross[26], J. Grunhaus[23], M. Gruwé[27], C. Hajdu[31] G.G. Hanson[12], M. Hansroul[8], M. Hapke[13], K. Harder[27], A. Harel[22], C.K. Hargrove[7], M. Harin-Dirac[4], M. Hauschild[8], C.M. Hawkes[1], R. Hawkings[27], R.J. Hemingway[6], G. Herten[10], R.D. Heuer[27], M.D. Hildreth[8], J.C. Hill[5], P.R. Hobson[25], A. Hocker[9], K. Hoffman[8], R.J. Homer[1], A.K. Honma[28,a], D. Horváth[31,c], K.R. Hossain[30], R. Howard[29], P. Hüntemeyer[27], P. Igo-Kemenes[11], D.C. Imrie[25], K. Ishii[24], F.R. Jacob[20], A. Jawahery[17], H. Jeremie[18], M. Jimack[1], C.R. Jones[5], P. Jovanovic[1], T.R. Junk[6], N. Kanaya[24], J. Kanzaki[24], D. Karlen[6], V. Kartvelishvili[16], K. Kawagoe[24], T. Kawamoto[24], P.I. Kayal[30], R.K. Keeler[28], R.G. Kellogg[17], B.W. Kennedy[20], D.H. Kim[19], A. Klier[26], T. Kobayashi[24], M. Kobel[3,d], T.P. Kokott[3], M. Kolrep[10], S. Komamiya[24], R.V. Kowalewski[28], T. Kress[4], P. Krieger[6], J. von Krogh[11], T. Kuhl[3], P. Kyberd[13], G.D. Lafferty[16], H. Landsman[22], D. Lanske[14], J. Lauber[15], I. Lawson[28], J.G. Layter[4], D. Lellouch[26], J. Letts[12], L. Levinson[26], R. Liebisch[11], B. List[8], C. Littlewood[5], A.W. Lloyd[1], S.L. Lloyd[13], F.K. Loebinger[16], G.D. Long[28], M.J. Losty[7], J. Lu[29], J. Ludwig[10], D. Liu[12], A. Macchiolo[18], A. Macpherson[30], W. Mader[3], M. Mannelli[8], S. Marcellini[2], A.J. Martin[13], J.P. Martin[18], G. Martinez[17], T. Mashimo[24], P. Mättig[26], W.J. McDonald[30], J. McKenna[29], E.A. Mckigney[15], T.J. McMahon[1], R.A. McPherson[28], F. Meijers[8], P. Mendez-Lorenzo[33], F.S. Merritt[9], H. Mes[7], A. Michelini[2], S. Mihara[24], G. Mikenberg[26], D.J. Miller[15], W. Mohr[10], A. Montanari[2], T. Mori[24], K. Nagai[8], I. Nakamura[24], H.A. Neal[12,g], R. Nisius[8], S.W. O'Neale[1], F.G. Oakham[7], F. Odorici[2], H.O. Ogren[12], A. Okpara[11], M.J. Oreglia[9], S. Orito[24], G. Pásztor[31], J.R. Pater[16], G.N. Patrick[20], J. Patt[10], R. Perez-Ochoa[8], S. Petzold[27], P. Pfeifenschneider[14], J.E. Pilcher[9], J. Pinfold[30], D.E. Plane[8], P. Poffenberger[28], B. Poli[2], J. Polok[8], M. Przybycień[8,e], A. Quadt[8], C. Rembser[8], H. Rick[8], S. Robertson[28], S.A. Robins[22], N. Rodning[30], J.M. Roney[28], S. Rosati[3], K. Roscoe[16], A.M. Rossi[2], Y. Rozen[22], K. Runge[10], O. Runolfsson[8], D.R. Rust[12], K. Sachs[10], T. Saeki[24], O. Sahr[33], W.M. Sang[25], E.K.G. Sarkisyan[23], C. Sbarra[29], A.D. Schaile[33], O. Schaile[33], P. Scharff-Hansen[8], J. Schieck[11], S. Schmitt[11], A. Schöning[8], M. Schröder[8], M. Schumacher[3], C. Schwick[8], W.G. Scott[20], R. Seuster[14], T.G. Shears[8], B.C. Shen[4], C.H. Shepherd-Themistocleous[5], P. Sherwood[15], G.P. Siroli[2], A. Sittler[27], A. Skuja[17], A.M. Smith[8], G.A. Snow[17], R. Sobie[28], S. Söldner-Rembold[10,f], S. Spagnolo[20], M. Sproston[20], A. Stahl[3], K. Stephens[16], J. Steuerer[27], K. Stoll[10], D. Strom[19], R. Ströhmer[33], B. Surrow[8], S.D. Talbot[1], P. Taras[18], S. Tarem[22], R. Teuscher[9], M. Thiergen[10], J. Thomas[15], M.A. Thomson[8], E. Torrence[8], S. Towers[6],

I. Trigger[18], Z. Trócsányi[32], E. Tsur[23], A.S. Turcot[9], M.F. Turner-Watson[1], I. Ueda[24], R. Van Kooten[12], P. Vannerem[10], M. Verzocchi[8], H. Voss[3], F. Wäckerle[10], A. Wagner[27], C.P. Ward[5], D.R. Ward[5], P.M. Watkins[1], A.T. Watson[1], N.K. Watson[1], P.S. Wells[8], N. Wermes[3], D. Wetterling[11] J.S. White[6], G.W. Wilson[16], J.A. Wilson[1], T.R. Wyatt[16], S. Yamashita[24], V. Zacek[18], D. Zer-Zion[8]

[1]School of Physics and Astronomy, University of Birmingham, Birmingham B15 2TT, UK
[2]Dipartimento di Fisica dell' Università di Bologna and INFN, I-40126 Bologna, Italy
[3]Physikalisches Institut, Universität Bonn, D-53115 Bonn, Germany
[4]Department of Physics, University of California, Riverside CA 92521, USA
[5]Cavendish Laboratory, Cambridge CB3 0HE, UK
[6]Ottawa-Carleton Institute for Physics, Department of Physics, Carleton University, Ottawa, Ontario K1S 5B6, Canada
[7]Centre for Research in Particle Physics, Carleton University, Ottawa, Ontario K1S 5B6, Canada
[8]CERN, European Organisation for Particle Physics, CH-1211 Geneva 23, Switzerland
[9]Enrico Fermi Institute and Department of Physics, University of Chicago, Chicago IL 60637, USA
[10]Fakultät für Physik, Albert Ludwigs Universität, D-79104 Freiburg, Germany
[11]Physikalisches Institut, Universität Heidelberg, D-69120 Heidelberg, Germany
[12]Indiana University, Department of Physics, Swain Hall West 117, Bloomington IN 47405, USA
[13]Queen Mary and Westfield College, University of London, London E1 4NS, UK
[14]Technische Hochschule Aachen, III Physikalisches Institut, Sommerfeldstrasse 26-28, D-52056 Aachen, Germany
[15]University College London, London WC1E 6BT, UK
[16]Department of Physics, Schuster Laboratory, The University, Manchester M13 9PL, UK
[17]Department of Physics, University of Maryland, College Park, MD 20742, USA
[18]Laboratoire de Physique Nucléaire, Université de Montréal, Montréal, Quebec H3C 3J7, Canada
[19]University of Oregon, Department of Physics, Eugene OR 97403, USA
[20]CLRC Rutherford Appleton Laboratory, Chilton, Didcot, Oxfordshire OX11 0QX, UK
[22]Department of Physics, Technion-Israel Institute of Technology, Haifa 32000, Israel
[23]Department of Physics and Astronomy, Tel Aviv University, Tel Aviv 69978, Israel
[24]International Centre for Elementary Particle Physics and Department of Physics, University of Tokyo, Tokyo 113-0033, and Kobe University, Kobe 657-8501, Japan
[25]Institute of Physical and Environmental Sciences, Brunel University, Uxbridge, Middlesex UB8 3PH, UK
[26]Particle Physics Department, Weizmann Institute of Science, Rehovot 76100, Israel
[27]Universität Hamburg/DESY, II Institut für Experimental Physik, Notkestrasse 85, D-22607 Hamburg, Germany
[28]University of Victoria, Department of Physics, P O Box 3055, Victoria BC V8W 3P6, Canada
[29]University of British Columbia, Department of Physics, Vancouver BC V6T 1Z1, Canada
[30]University of Alberta, Department of Physics, Edmonton AB T6G 2J1, Canada
[31]Research Institute for Particle and Nuclear Physics, H-1525 Budapest, P O Box 49, Hungary
[32]Institute of Nuclear Research, H-4001 Debrecen, P O Box 51, Hungary

[33]Ludwigs-Maximilians-Universität München, Sektion Physik, Am Coulombwall 1, D-85748 Garching, Germany

[a] and at TRIUMF, Vancouver, Canada V6T 2A3
[b] and Royal Society University Research Fellow
[c] and Institute of Nuclear Research, Debrecen, Hungary
[d] on leave of absence from the University of Freiburg
[e] and University of Mining and Metallurgy, Cracow
[f] and Heisenberg Fellow
[g] now at Yale University, Dept of Physics, New Haven, USA
[h] and Department of Experimental Physics, Lajos Kossuth University, Debrecen, Hungary.

1 Introduction

We present a search for a di-photon resonance produced in e^+e^- collisions at LEP. The data were taken by the OPAL detector at centre-of-mass energies $E_{\rm cm}$ up to 189 GeV. The search is sensitive to the process $e^+e^- \to XY$, with $X \to \gamma\gamma$ and $Y \to f\bar{f}$, where $f\bar{f}$ may be quarks, charged leptons, or a neutrino pair. In a Standard Model scenario, Y is a Z^0 and X is a Higgs boson decaying into two photons. A more general search is achieved by removing the restriction that Y is a Z^0.

In the minimal Standard Model, the single Higgs boson can decay into two photons via a quark- or W-boson loop [1]. The rate is too small for observation at existing accelerators even for a kinematically accessible Higgs boson, but other theoretical models can accommodate large $h^0 \to \gamma\gamma$ branching ratios [2]. Throughout this paper, "h^0" refers to a neutral CP-even scalar where non-minimal Higgs sector models are discussed. Particularly interesting are non-minimal Higgs sectors wherein some Higgs components couple only to bosons [3]. This class of "fermiophobic" Higgs models includes the "Bosonic" Higgs model [4], and Type I Two-Higgs Doublet models with fermiophobic couplings [5]. In Higgs triplet models [6], the particles formed from the triplet fields are fermiophobic.

There are existing limits on the production of a di-photon resonance which couples to the Z^0. Using data taken up to $E_{\rm cm}$=183 GeV, OPAL has set upper limits on the branching ratio $h^0 \to \gamma\gamma$ for masses up to 92 GeV [7, 8] and obtained a 95% confidence level (CL) lower mass limit of 90.0 GeV for a fermiophobic Higgs scalar. Other collaborations [9, 10] have recently reported limits on photonic Higgs boson decays. The lower mass region ($M_{\gamma\gamma}<$ 60 GeV) has been searched previously using data from LEP-I [11, 12, 13].

2 Data and Monte Carlo Samples

The analysis is performed on the data collected with the OPAL detector [14] during the 1998 LEP run. The data sample corresponds to an integrated luminosity of 182.6 ± 0.8 pb^{-1} collected at a luminosity-weighted $E_{\rm cm}$ of 188.63 ± 0.04 GeV.

To assess the sensitivity of the analysis to signals, two production models are considered: the Standard Model process $e^+e^- \to h^0Z^0$, and Two Higgs Doublet models (2HDM) for $e^+e^- \to h^0A^0$. The process $e^+e^- \to h^0Z^0$, $h^0 \to \gamma\gamma$ was simulated for each Z^0 decay channel using the HZHA generator [15]. For the general search, mass grids were generated using the $e^+e^- \to h^0Z^0$ and $e^+e^- \to h^0A^0$ processes as models for $e^+e^- \to XY,\ X \to \gamma\gamma,\ Y \to f\bar{f}$.

The dominant background to this search arises from the emission of two energetic initial state radiation (ISR) photons in hadronic events from $e^+e^- \to (\gamma/Z)^* \to q\bar{q}$. This process was simulated using the KK2f generator using CEEX [16] ISR modelling, and with the set of hadronization parameters described in reference [17]. Other Standard Model backgrounds, particularly those from 4-fermion processes, primarily affect the leptonic and missing energy modes of the search. Four-fermion processes were modelled using the Vermaseren [18] and grc4f [19] generators implemented in the KORALW [20] Monte Carlo program. The programs BHWIDE [21] and TEEGG [22] were employed to model the s- and t-channel backgrounds from Bhabha scattering. The processes $e^+e^- \to \ell^+\ell^-$ with $\ell \equiv \mu, \tau$ were simulated using KORALZ [23]. The KORALZ program was also used to generate events of the type $e^+e^- \to$

$\nu\bar{\nu}\gamma(\gamma)$. The process $e^+e^- \to \gamma\gamma$ was simulated using the RADCOR generator [24]. Simulated events were processed using the full OPAL detector Monte Carlo [25] and analyzed in the same manner as the data.

3 Event Selection

In our searches for the generic process $e^+e^- \to XY$, we consider three event topologies which are motivated mainly by the particular case where X is a generic Higgs boson decaying into a pair of photons, and Y is the Z^0 boson decaying either into (1) a $q\bar{q}$ pair, or (2) a pair of oppositely charged leptons, or (3) a $\nu\bar{\nu}$ pair. The search topologies are therefore:

- Two energetic photons recoiling against a hadronic system.
- Two energetic photons produced in association with charged leptons.
- Two energetic photons and no other significant detector activity.

In the h^0Z^0 search, the mass recoiling from the di-photon system is required to be consistent with the Z^0 mass for all topologies, while in the general search this condition is not required. A background common to all search modes arises from events with two visible ISR photons, resulting in an on-shell Z^0 recoiling from a di-photon system.

The selection criteria employed in this search are very similar to those described in reference [7]. For all topologies, charged tracks (CT) and unassociated electromagnetic calorimeter (EC) clusters are required to satisfy the criteria defined in reference [26]. "Unassociated" EC clusters are defined by the requirement that no charged tracks point to the cluster. For each channel, preselection cuts are applied which employ the following measured quantities:

- $E_{\rm vis}$ and $\vec{p}_{\rm vis}$: the scalar and vector sums of charged track momenta, unassociated EC and unassociated hadron calorimeter cluster energies.
- $R_{\rm vis} \equiv \dfrac{E_{\rm vis}}{E_{\rm cm}}$.
- Visible momentum along the beam direction: $|\Sigma\ p_z^{\rm vis}|$, where all tracks and unassociated clusters are summed over.

3.1 Photon Pair Identification

After channel-dependent preliminary cuts based on data quality and rudimentary event topology (described in the next sections), events are required to have a photon pair satisfying several criteria. Photon identification is accomplished by identifying clusters in the electromagnetic calorimeter. These EC clusters are combined with the information from the tracking detectors to identify photon candidates if the lateral spread of the clusters satisfies the criteria described in reference [8]. The photon detection efficiency is increased by including photon conversions into e^+e^- pairs using the methods described in reference [7].

The most significant background to all search channels are processes having two ISR photons. Photons from ISR are peaked along the beam direction, hence cutting on the photon polar angle $|\cos(\theta_\gamma)| < 0.875$ is very effective in reducing the background acceptances without significantly decreasing the efficiencies for potential signals. Figure 1 shows the distribution of $E_{\gamma 1}$, the highest-energy photon, in events having hadronic activity (criterion A1 described below), where at least one photon has $E_\gamma > 0.05 \times E_{\rm beam}$ and $|\cos(\theta_\gamma)| < 0.875$. Also shown is the simulated Standard Model background. The overall number of background photons, their energies, and their polar angle distribution (not shown) describe the data to better than 10%. The photon pair acceptance criteria is thus summarized by the following requirements on the two highest-energy photons in the event:

- The two photon candidates are required to be in the fiducial region $|\cos(\theta_\gamma)| < 0.875$, where θ_γ is the angle of the photon with respect to the e^- beam direction.
- The higher energy photon is required to have $E_\gamma/E_{\rm beam} > 0.10$ and the second-highest-energy photon is required to have $E_\gamma/E_{\rm beam} > 0.05$.

After the final channel cuts described in the next sections, there are no events in which more than one photon pair is found.

3.2 Hadronic Channel

The hadronic channel is characterized by two photons recoiling against a hadronic system. In addition to double ISR, backgrounds also arise from radiative $Z^0\gamma$ events where a decay product of the Z^0, such as an isolated π^0 or η meson, mimics a photon, or there is an energetic final state radiation (FSR) photon. In these cases, the recoil mass against the di-photon system will tend to be lower than the Z^0 mass; therefore, this background can be suppressed by requiring a recoil mass consistent with that of the Z^0. In the general search for $XY \to \gamma\gamma$ + hadrons, there is no recoil mass constraint to help suppress backgrounds from fake photons.

The hadronic channel candidate selection is summarized in Table 1. Candidate events are required to satisfy the following criteria:

(A1) The standard hadronic event preselection described in reference [27] with the additional requirements:
  - $R_{\rm vis} > 0.5$ and $|\Sigma\ p_z^{\rm vis}| < 0.6 E_{\rm beam}$;
  - at least 2 electromagnetic clusters with $E/E_{\rm beam} > 0.05$.

(A2) The photon pair criteria described in Section 3.1.

(A3) To suppress the background from FSR and fake photons, the charged tracks and unassociated clusters were grouped into two jets using the Durham scheme [28], excluding the photon candidates. Both photon candidates are then required to satisfy $p_{\rm T,\ jet-\gamma} > 5$ GeV, where $p_{\rm T,\ jet-\gamma}$ was defined as the photon momentum transverse to the axis defined by the closest jet.

In the case of double ISR emission in the hadron channel, the photons tend to have a large energy difference. We therefore employ the quantity $\Delta E = (E_{\gamma 1} - E_{\gamma 2})/\mathrm{E_o}$, where $E_{\gamma 1}$ and $E_{\gamma 2}$ are the first- and second-highest-energy photons in the event, and $\mathrm{E_o} = (\mathrm{E_{cm}}^2 - \mathrm{M_Z^2})/(2\mathrm{E_{cm}})$ is the energy of a single photon recoiling from the $\mathrm{Z^0}$.

(A4) $\Delta E < 0.5$.

(A5) For the $\mathrm{h^0Z^0}$ topology, the invariant mass recoiling from the di-photon must satisfy $|M_{\mathrm{recoil}} - M_{\mathrm{Z}}| < 20$ GeV.

For the general search topology, where no explicit recoil mass cut is made, 16 events are observed, while 17.4 ± 1.7 are expected from Standard Model backgrounds. The uncertainty shown is for Monte Carlo statistics only [1]. After applying the cut (A5) on the recoil mass, 10 events remain, compared to an expectation of 9.0 ± 1.3 events. The efficiencies for this analysis to accept events for Higgs masses of 30 to 100 GeV are shown in Table 4.

3.3 Charged Lepton Channel

This channel searches for events in the $\gamma\gamma\ell^+\ell^-$ final state. Even in the case of $\ell = \tau$, this channel has a very clean signature, and therefore only one selection procedure is required for the e, μ and τ channels. Charged leptons are identified as low multiplicity jets formed from charged tracks and isolated EC clusters. A high efficiency is maintained for τ leptons by allowing single charged tracks to define a "jet" without requiring explicit lepton identification. This channel is sufficiently free of background to allow acceptance of events where one of the charged leptons was not reconstructed or was lost in uninstrumented regions of the detector. The most serious background comes from Bhabha scattering with initial and/or final state radiation.

The leptonic channel event selection is summarized in Table 2. Leptonic channel candidates are required to satisfy the following criteria:

(B1) The low multiplicity preselection of reference [29] and:

- $R_{\mathrm{vis}} > 0.2$ and $|\Sigma\ p_z^{\mathrm{vis}}| < 0.8 E_{\mathrm{beam}}$;
- number of EC clusters not associated with tracks: $N_{\mathrm{EC}} \leq 10$;
- number of charged tracks: $1 \leq N_{\mathrm{CT}} \leq 7$;
- at least 2 electromagnetic clusters with $E/E_{\mathrm{beam}} > 0.05$.

(B2) The photon pair criteria described in Section 3.1.

(B3) For events having only one charged track, require:

- the track not to be associated with a converted photon;
- the track to have momentum satisfying $p > 0.2 E_{\mathrm{beam}}$;
- direction of event missing momentum: $|\cos\theta_{\mathrm{miss}}| > 0.90$.

[1] Unless otherwise specified, all errors quoted are statistical only.

(B4) For events having two or more charged tracks, the event is forced to have 2 jets within the Durham scheme, excluding the identified di-photon candidate.

(B5) For the h^0Z^0 search, the recoil mass to the di-photon is required to be consistent with the Z^0: $|M_{\rm recoil} - M_{\rm Z}| < 20$ GeV.

For the general search, 20 events survive cuts B1-B4, compared to 25.6 ± 1.6 expected from Standard Model backgrounds. After the recoil mass requirement, the number of observed events is 7, with the background expectation of 8.9 ± 1.0. The efficiencies for Higgs masses of 30 to 100 GeV are given in Table 4.

3.4 Missing Energy Channel

The missing energy channel is characterized by two photons and no other significant detector activity. An irreducible Standard Model background is the process $e^+e^- \to \nu\bar{\nu}\gamma\gamma$. Other potential backgrounds include $e^+e^- \to \gamma\gamma(\gamma)$ and radiative Bhabha scattering with one or more unobserved electrons. These backgrounds tend to produce photons near the beam directions; therefore, they can be effectively dealt with by the restriction on the polar angles of the two photons and by requiring consistency with a di-photon recoiling from a massive object.

The event selection for the missing energy channel is summarized in Table 3. Candidates in the missing energy channel are required to satisfy the following criteria:

(C1) The low multiplicity preselection of reference [29] with the further requirement that the event satisfy the cosmic ray and beam-wall/beam-gas vetoes described in reference [30], and:

- number of EC clusters not associated with tracks: $N_{\rm EC} \leq 4$;
- number of charged tracks: $N_{\rm NCT} \leq 3$;
- $|\Sigma\ p_z^{\rm vis}| < 0.8 E_{\rm beam}$;
- at least 2 electromagnetic clusters with $E/E_{\rm beam} > 0.05$.

(C2) The photon pair criteria described in Section 3.1.

(C3) Consistency with the hypothesis that the di-photon system is recoiling from a massive body:

- The momentum component of the di-photon system in the plane transverse to the beam axis: $p_T(\gamma\gamma) > 0.05 E_{\rm beam}$.
- The angle between the two photons in the plane transverse to the beam axis: $|\phi_{\gamma\gamma} - 180^\circ| > 2.5^\circ$.
- The polar angle of the momentum of the di-photon system: $|\cos\theta_{\gamma\gamma}| < 0.966$.

(C4) Events are required to have no charged track candidates (other than those associated with an identified photon conversion).

(C5) Veto on unassociated calorimeter energy: the energy observed in the electromagnetic calorimeter not associated with the 2 photons is required to be less than 3 GeV.

(C6) For the h^0Z^0 search, the recoil mass against the di-photon is required to be consistent with the Z^0: $|M_{\rm recoil} - M_{\rm Z}| < 20$ GeV.

The number of events passing the general cuts C1-C5 is 8, compared to the Standard Model background expectation of 11.2 ± 0.5. After application of the recoil mass cut (C6), 5 candidates remain compared to an expectation of 7.1 ± 0.3 events from Standard Model sources. The efficiencies for Higgs masses from 30 to 100 GeV are summarized in Table 4.

3.5 Systematic Errors

The dominant systematic uncertainty for acceptances arises from the photon detection efficiency, primarily due to the simulation of the photon isolation criteria [11]. This uncertainty is estimated to be 3% of the acceptance from comparison of data with Standard Model backgrounds. Photon energies and angles are well measured and consequently lead to a systematic uncertainty on the efficiencies of 0.6%, as determined from the measured di-photon recoil mass distribution. The systematic error on the integrated luminosity of the data is 0.4% and contributes negligibly to the limits. The uncertainty from simulation Monte Carlo statistics is typically better than 4%. From the differences observed in the comparison of data and simulations of Standard Model backgrounds (particularly the KK2f modelling of ISR), the systematic uncertainty for backgrounds is taken to be 10%; this value is subtracted from the predicted background in the setting of limits. A systematic error on the photon energy scale is estimated to be 0.25 GeV for 72 GeV photons using the fitted single-photon ISR peak in Figure 1 compared to the expected value based on the precisely known beam energy and Z^0 mass. This leads to a systematic uncertainty on the di-photon mass of 0.35 GeV at a mass of 100 GeV.

The background events in the missing energy channel include a component from Compton scattering in the beams, which is modelled by the TEEGG Monte Carlo. The photons from this process have a high probability to be found in the near the cut on polar angle. The photon energy uncertainty is rather large (5-9 GeV) in these regions because of the corrections for passage through significant material.

4 Results

Figure 2 shows the di-photon mass versus the recoil mass for all candidate events passing the general search cuts. The distribution of di-photon masses for the h^0Z^0 search candidates is shown in Figure 3, together with the simulation of Standard Model backgrounds. Combining all three general search channels results in 44 observed events versus 54.2 ± 2.5 expected from Standard Model sources. Summing over all three h^0Z^0 channel decay modes and expected background sources yields 25.0 ± 1.7 events expected versus 22 observed.

4.1 General Search Results

Using only the data taken at $E_{\rm cm}$=189 GeV, we set limits for the production mode $e^+e^- \to XY$, where X is any scalar resonance decaying into di-photons. The candidate events from the

general search (no recoil mass cut) are used to set upper limits on $\sigma(e^+e^- \to XY) \times B(X \to \gamma\gamma) \times B(Y \to f\bar{f})$. Such results are valid independent of the nature of Y, provided it decays to a fermion pair and has negligible width. The search is also restricted to X and Y masses above 10 GeV and below 180 GeV in order to allow the decay products to have sufficient energies and momenta to give reasonable search acceptances.

The event candidates from the general search are used to calculate 95% CL upper limits on the number of events in 1 GeV $[M_X, M_Y]$ mass bins, where M_X corresponds to the di-photon mass and M_Y to the recoil mass. Efficiencies for signals were calculated using two grids of simulated signals which were interpolated from Monte Carlo samples generated in 10 GeV $[M_X, M_Y]$ steps using the $e^+e^- \to h^0Z^0$ and the $e^+e^- \to h^0A^0$ processes as models for the $e^+e^- \to XY \to \gamma\gamma + f\bar{f}$ final state. The grid was generated for X masses from 10 to 180 GeV and Y masses from 10 to 180 GeV such that $M_X + M_Y > M_Z$. This latter constraint was motivated by the higher sensitivity of searches performed at $E_{cm}=M_Z$. For each $[M_X, M_Y]$ bin, the 95% CL upper limit on the number of signal events is computed using the frequentist method of reference [31]. This statistical procedure incorporates the di-photon mass resolution (typically less than 2 GeV for $M_{\gamma\gamma}<100$ GeV). The effect of the systematic error for efficiencies and background modelling is incorporated by reducing the subtracted background by the systematic, but using an additional systematic uncertainty of 5% to account for interpolation error in the efficiency grid (especially near kinematic limits).

Figure 4 shows the 95% CL upper limits on $\sigma(e^+e^- \to XY) \times B(X \to \gamma\gamma) \times B(Y \to f\bar{f})$. To present the limits only as a function of M_X, the figure shows the weakest limit obtained in each M_X bin as M_Y was scanned subject to the constraints mentioned above. For a scalar/vector hypothesis for X/Y, the efficiency is found to be the same to within 5% with that for a scalar/scalar hypothesis; the lower of these efficiencies is used in setting the limits. For the lepton search channel, the efficiency for $Y \to \tau^+\tau^-$ is used, as it turns out to have the lowest of the dilepton efficiencies. Cross section limits of 30 – 100 fb are obtained over $10 < M_X < 180$ GeV.

4.2 Search for the Standard Model Higgs Boson

The events passing all h^0Z^0 cuts are used to set an upper limit on the di-photon branching ratio of a particle having the Standard Model Higgs boson production rate. For each 1 GeV di-photon mass bin, the 95% CL upper limit on the number of signal events is computed using the frequentist method and background subtraction as in the previous section, with the efficiencies now including the Standard Model Z^0 branching fractions. Figure 5 shows the 95% CL upper limit for the di-photon branching ratio obtained by combining the E_{cm}=189 GeV candidate events with those from OPAL searches at E_{cm}=91–183 GeV [7, 8, 11], where the Standard Model $h^0Z^{0(*)}$ production cross section is assumed at each E_{cm}. For masses lower than approximately 60 GeV, LEP-1 limits for $B(h^0 \to \gamma\gamma)$ have been inferred from references [11, 12].

The limits on $B(h^0 \to \gamma\gamma)$ are used to rule out Higgs bosons in certain non-minimal models. Shown in Figure 5 is the $h^0 \to \gamma\gamma$ branching ratio in the Standard Model computed using HDECAY [32] with the fermionic couplings switched off. A 95% CL lower mass limit for such fermiophobic Higgs bosons is set at 96.2 GeV, where the predicted branching ratio crosses the upper-limit curve.

4.3 The Higgs Triplet Model

It is possible that a non-minimal Higgs sector incorporates triplet fields; particles formed exclusively from such fields are fermiophobic. The minimal Higgs Triplet model (HTM) [33, 34] requires the inclusion of two triplet fields in order to have the ρ-parameter near unity. The model has 10 Higgs bosons in the form of a fiveplet (H_5), a threeplet (H_3), and two singlets (H_1). The H_5^0 and one of the singlets, $H_1^{0'}$, are formed from the triplet field, apart from possible mixing with doublet components. Akeroyd [34] has shown that measurements constrain the mixing parameters so that the $H_1^{0'}$ is almost entirely fermiophobic, and therefore could be interpreted as the X in this search.

The process $e^+e^- \to H_1^{0'}Z^0$ occurs at the Standard Model h^0Z^0 rate modified by the factor $\frac{8}{3}\sin^2\theta_H$, where the angle θ_H is a parameter of the model describing the mixing of the doublet and triplet fields. Limits on θ_H can therefore be inferred from Figure 5 by dividing the upper limit by the fermiophobic di-photon branching ratio. The limits on θ_H obtained from this experiment are more restrictive than limits inferred from the Z^0 width [34] up to an $H_1^{0'}$ mass of approximately 96 GeV.

5 Conclusions

A search for the production of Higgs bosons and other new particles decaying to photon pairs has been performed using 182.6 pb^{-1} of data taken at an average centre-of-mass energy of 188.6 GeV. Model independent upper limits are obtained on $\sigma(e^+e^- \to XY) \times B(X \to \gamma\gamma) \times B(Y \to f\bar{f})$. Limits of 30 – 100 fb are obtained over $10 < M_X < 180$ GeV, where $10 < M_Y < 180$ GeV and $M_X + M_Y > M_Z$, for Y either a scalar or vector particle, provided that the Y decays to a fermion pair.

The results of this search have been combined with previous OPAL results to set limits on $B(h^0 \to \gamma\gamma)$ up to a Higgs boson mass of 100 GeV, provided the Higgs particle is produced via $e^+e^- \to h^0Z^0$ at the Standard Model rate. A lower mass bound of 96.2 GeV is set at the 95% confidence level for Higgs particles which do not couple to fermions.

Acknowledgements

We particularly wish to thank the SL Division for the efficient operation of the LEP accelerator at all energies and for their continuing close cooperation with our experimental group. We thank our colleagues from CEA, DAPNIA/SPP, CE-Saclay for their efforts over the years on the time-of-flight and trigger systems which we continue to use. In addition to the support staff at our own institutions we are pleased to acknowledge the
Department of Energy, USA,
National Science Foundation, USA,
Particle Physics and Astronomy Research Council, UK,
Natural Sciences and Engineering Research Council, Canada,
Israel Science Foundation, administered by the Israel Academy of Science and Humanities,
Minerva Gesellschaft,
Benoziyo Center for High Energy Physics,

Japanese Ministry of Education, Science and Culture (the Monbusho) and a grant under the Monbusho International Science Research Program,
Japanese Society for the Promotion of Science (JSPS),
German Israeli Bi-national Science Foundation (GIF),
Bundesministerium für Bildung, Wissenschaft, Forschung und Technologie, Germany,
National Research Council of Canada,
Research Corporation, USA,
Hungarian Foundation for Scientific Research, OTKA T-016660, T023793 and OTKA F-023259.

References

[1] J. Ellis, M.K. Gaillard, and D.V. Nanopoulos, Nucl. Phys. **B106** (1976) 292.

[2] K. Hagiwara and M.L. Stong, Z. Phys. **C62** (1994) 99.

[3] A.G. Akeroyd, Phys. Lett. **B368** (1996) 89.

[4] A. Stange, W. Marciano and S. Willenbrock, Phys. Rev. **D49** (1994) 1354.

[5] H. Haber, G. Kane and T. Sterling, Nucl. Phys. **B161** (1979) 493.

[6] J.F. Gunion, R. Vega and J. Wudka, Phys. Rev. **D42** (1990) 1673.

[7] OPAL Collab., K. Ackerstaff *et al.*, Phys. Lett. **B437** (1998) 218.

[8] OPAL Collab., K. Ackerstaff *et al.*, Eur. Phys. J. **C1** (1998) 31.

[9] B. Abbott *et al.*, Phys. Rev. Lett. **82** (1999) 2244.

[10] DELPHI Collab., P. Abreu *et al.*, CERN-EP/99-58 (1999), accepted by Phys. Lett. **B**.

[11] OPAL Collab., G. Alexander *et al.*, Z. Phys. **C71** (1996) 1.

[12] L3 Collab., M. Acciarri *et al.*, Phys. Lett. **388** (1996) 409;
DELPHI Collab., P. Abreu *et al.*, Z. Phys. **C72** (1996) 179.

[13] OPAL Collab., P. Acton *et al.*, Phys. Lett. **311** (1993) 391;
ALEPH Collab., D. Buskulic *et al.*, Phys. Lett. **B313** (1993) 299;
L3 Collab., O. Adriani *et al.*, Phys. Lett. **295** (1992) 337.

[14] OPAL Collab., K. Ahmet *et al.*, Nucl. Instr. Meth. **A305** (1991) 275;
O. Biebel *et al.*, Nucl. Instr. Meth. **A323** (1992) 169;
M. Hauschild *et al.*, Nucl. Instr. Meth. **A314** (1992) 74;
S. Anderson *et al.*, Nucl. Instr. Meth. **A403** (1998) 326.

[15] HZHA generator: P. Janot, in *Physics at LEP2,* edited by G. Altarelli, T. Sjöstrand and F. Zwirner, CERN 96-01 Vol. 2 p.309.

[16] S. Jadach, B.F. Ward and Z. Was, "Coherent exclusive exponentiation CEEX: the case of the resonant e^+e^- collision" CERN-TH-98-253.

[17] OPAL Collab., G. Alexander *et al.*, Z. Phys. **C69** (1996) 543.

[18] J.A.M. Vermaseren, Nucl. Phys. **B229** (1983) 347.

[19] J. Fujimoto et al., Comp. Phys. Comm. **100** (1997) 128.

[20] M. Skrzypek *et al.*, Comp. Phys. Comm. **94** (1996) 216;
M. Skrzypek *et al.*, Phys. Lett. **B372** (1996) 289.

[21] S. Jadach, W. Placzek and B. F. L. Ward, University of Tennessee preprint, UTHEP 95-1001 (unpublished).

[22] D. Karlen, Nucl. Phys. **B289** (1987) 23.

[23] S. Jadach et al., Comp. Phys. Comm. **66** (1991) 276.

[24] F.A. Berends and R. Kleiss, Nucl. Phys. **B186** (1981) 22.

[25] J. Allison *et al.*, Nucl. Instr. Meth. **A305** (1992) 47.

[26] OPAL Collab., G. Alexander *et al.*, Z. Phys. **C72** (1996) 191.

[27] OPAL Collab., G. Alexander *et al.*, Z. Phys. **C52** (1991) 175.

[28] N. Brown and W.J. Stirling, Phys. Lett. **B252** (1990) 657;
S. Bethke, Z. Kunszt, D. Soper and W.J. Stirling, Nucl. Phys. **B370** (1992) 310;
S. Catani *et al.*, Phys. Lett. **B269** (1991) 432;
N. Brown and W.J. Stirling, Z. Phys. **C53** (1992) 629.

[29] OPAL Collab., R. Akers *et al.*, Z. Phys. **C61** (1994) 19.

[30] OPAL Collab., R. Akers *et al.*, Z. Phys. **C65** (1995) 47.

[31] T. Junk, "Confidence Level Computation for Combining Searches with Small Statistics", CERN-EP/99-041, to appear in NIM **A**.

[32] A. Djouadi, J. Kalinowski and M. Spira, Comp. Phys. Comm. **108** (1998) 56.

[33] H. Georgi and M. Machacek, Nucl. Phys. **B262** (1985) 463.

[34] A.G. Akeroyd, Phys. Lett. **B353** (1995) 519.

Cut	Data	ΣBkgd	$(\gamma/Z)^*$	4f
(A1)	10075	10024.6	7321.0	2703.6
(A2)	63	54.0	51.6	2.4
(A3)	38	41.4	39.7	1.7
(A4)	16	17.4 ± 1.7	15.9	1.5
(A5)	10	9.0 ± 1.3	8.7	0.3

Table 1: Events remaining in the hadronic search channel after the indicated cumulative cuts described in Section 3.2. The entry for (A4) is used in the general search. The entry for (A5) is for the M_{recoil} cut for the h^0Z^0 search. In addition to the total simulated background (ΣBkgd), the components from $(\gamma/Z)^*$ and four-fermion ("4f") final states are shown.

Cut	Data	ΣBkgd	e^+e^-	$\tau^+\tau^-$	$\mu^+\mu^-$	$\gamma\gamma$	e^+e^-ff
(B1)	41115	36126.6	34679.8	646.9	36.3	281.1	482.4
(B2)	159	168.4	66.8	8.8	5.5	86.1	1.1
(B3)	146	161.6	62.1	8.3	5.2	84.9	1.1
(B4)	20	25.6 ± 1.8	16.2	3.9	5.0	0.2	0.3
(B5)	7	8.9 ± 1.0	4.7	1.5	2.5	0.0	0.1

Table 2: Events remaining for the leptonic channel analysis after the indicated cumulative cuts described in Section 3.3. In addition to the total simulated background (ΣBkgd), the individual contributions from Bhabha scattering (e^+e^-), τ-pair, μ-pair, $\gamma\gamma$ and $e^+e^-f\bar{f}$ final states are shown. Criterion (B5), the recoil mass cut, is only applied for the h^0Z^0 search.

Cut	Data	ΣBkgd	$\nu\bar{\nu}\gamma\gamma$	$\gamma\gamma$	e^+e^-	$\ell^+\ell^-$	e^+e^-ff
(C1)	213061	118393.4	40.9	2809.8	114303.6	141.3	1097.8
(C2)	323	287.9	11.3	232.7	42.9	0.7	0.3
(C3)	70	64.3	11.0	26.5	26.0	0.6	0.2
(C4)	34	36.1	10.8	24.6	0.6	0.0	0.1
(C5)	8	11.2 ± 0.5	10.4	0.3	0.4	0.0	0.1
(C6)	5	7.1 ± 0.3	7.0	0.0	0.0	0.0	0.1

Table 3: Events remaining after the indicated cumulative cuts for the missing energy search channel described in Section 3.4. In addition to the total simulated background (ΣBkgd), the individual contributions from $\nu\bar{\nu}\gamma\gamma$, $\gamma\gamma$, e^+e^--pair, lepton pair ($\ell \equiv \mu, \tau$) production and $e^+e^-f\bar{f}$ final states are shown. Criterion (C6), the recoil mass cut, is only applied for the h^0Z^0 search.

	Efficiency (%)									
	General Search					h^0Z^0 Search				
$M_{\gamma\gamma}$ (GeV):	30	50	70	90	100	30	50	70	90	100
$q\bar{q}\gamma\gamma$	35	37	39	39	38	29	35	46	57	49
$\ell\ell\gamma\gamma$	45	49	50	48	47	44	49	54	56	44
$\nu\bar{\nu}\gamma\gamma$	59	65	67	66	64	49	57	59	67	48

Table 4: Efficiency in percent (%) for each h^0Z^0 and general search channel for Higgs masses as indicated. The general search numbers indicate the minimum efficiency for variation of the recoil mass M_Y over $E_{cm} > M_X + M_Y > M_Z$, where M_X is the di-photon mass; the minimum general efficiency can therefore be smaller than the h^0Z^0 efficiency.

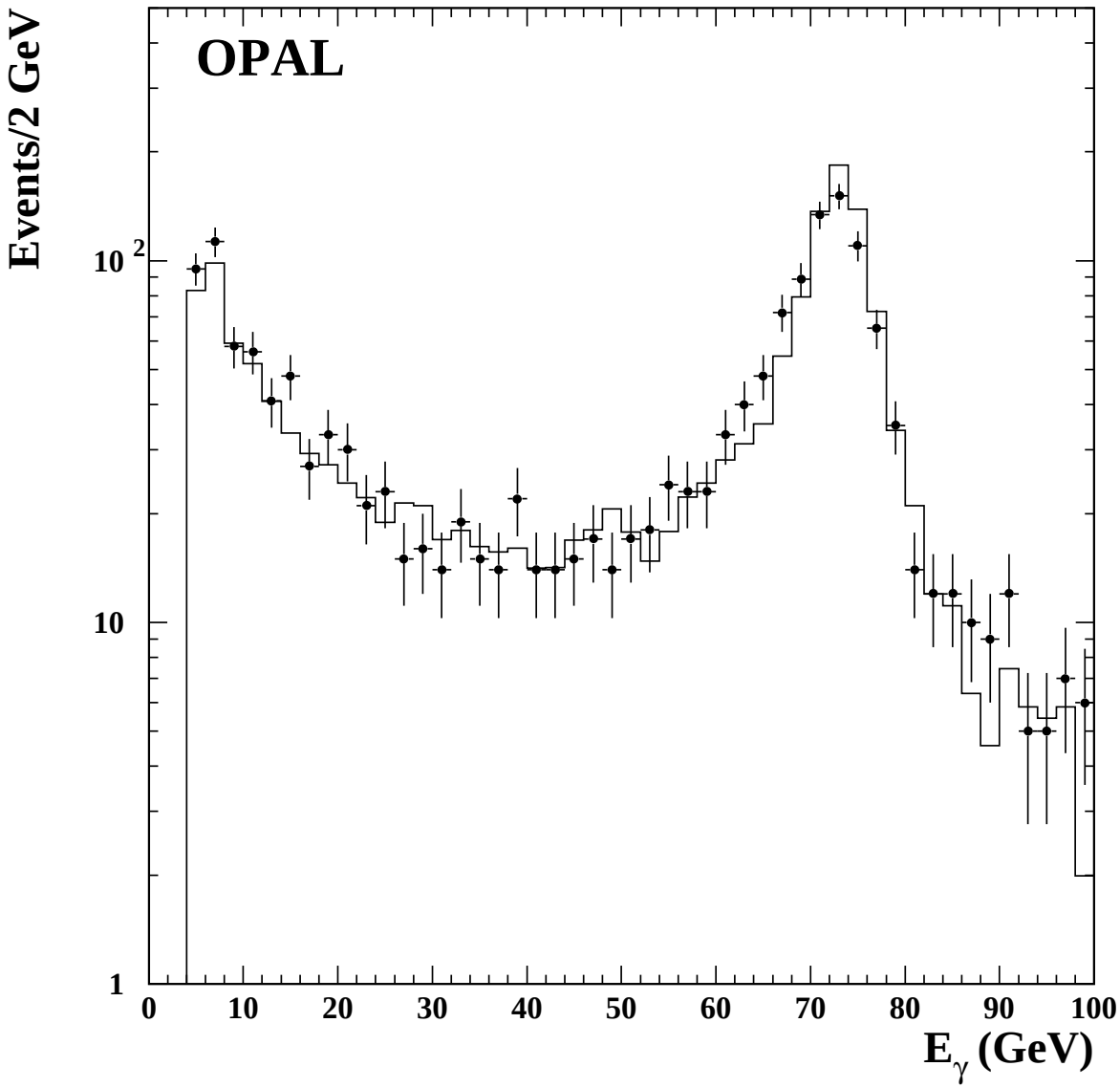

Figure 1: Energy distribution of highest-energy photon in the hadronic search channel. Data are shown as points with error bars. Background simulation is shown as a histogram.

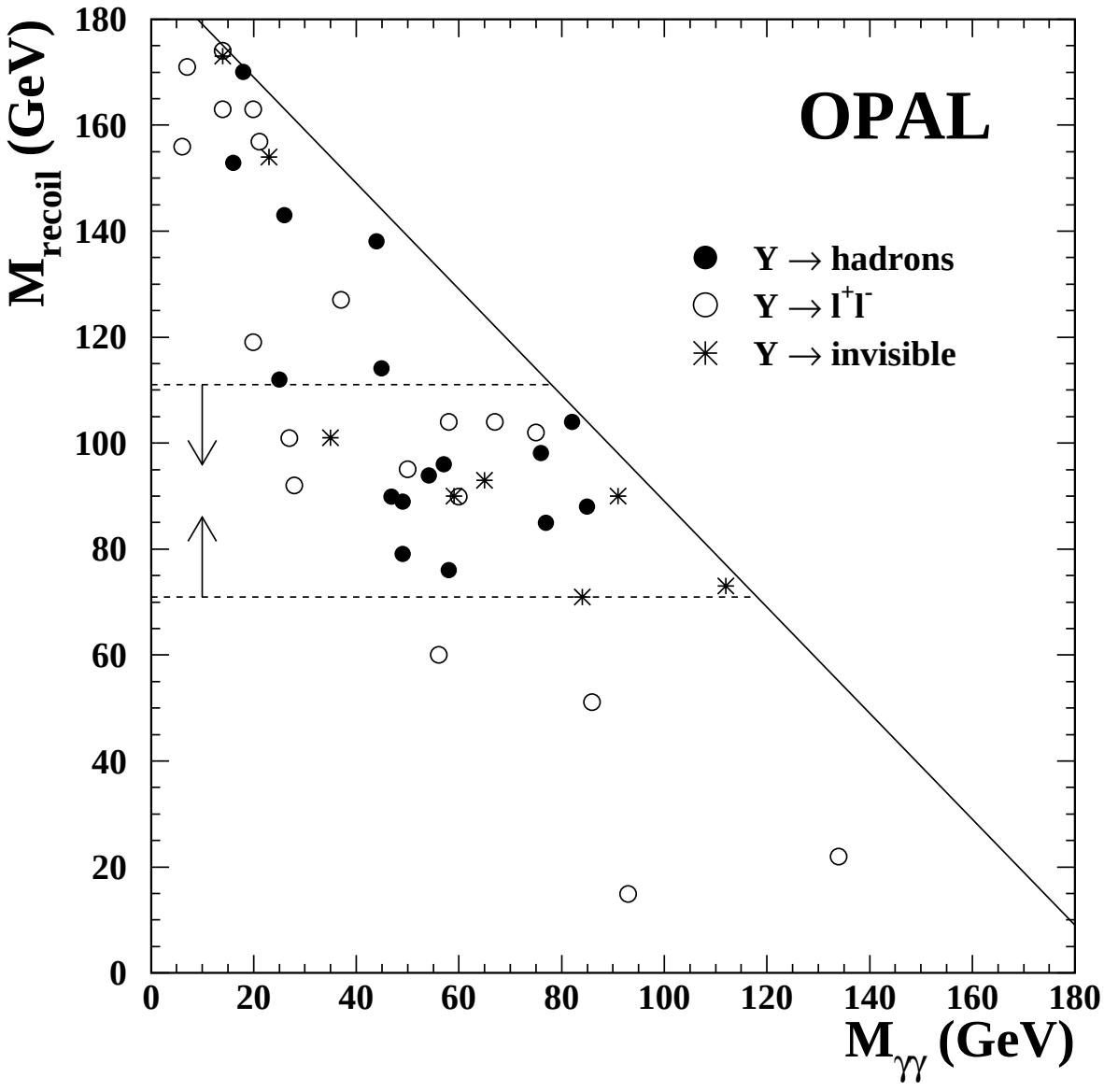

Figure 2: Distribution of mass recoiling against the di-photon system versus di-photon invariant mass for events passing the general search cuts. The different search channels are as indicated. The diagonal line denotes the kinematic limit. Dashed lines and arrows indicate the events accepted for the h^0Z^0 search.

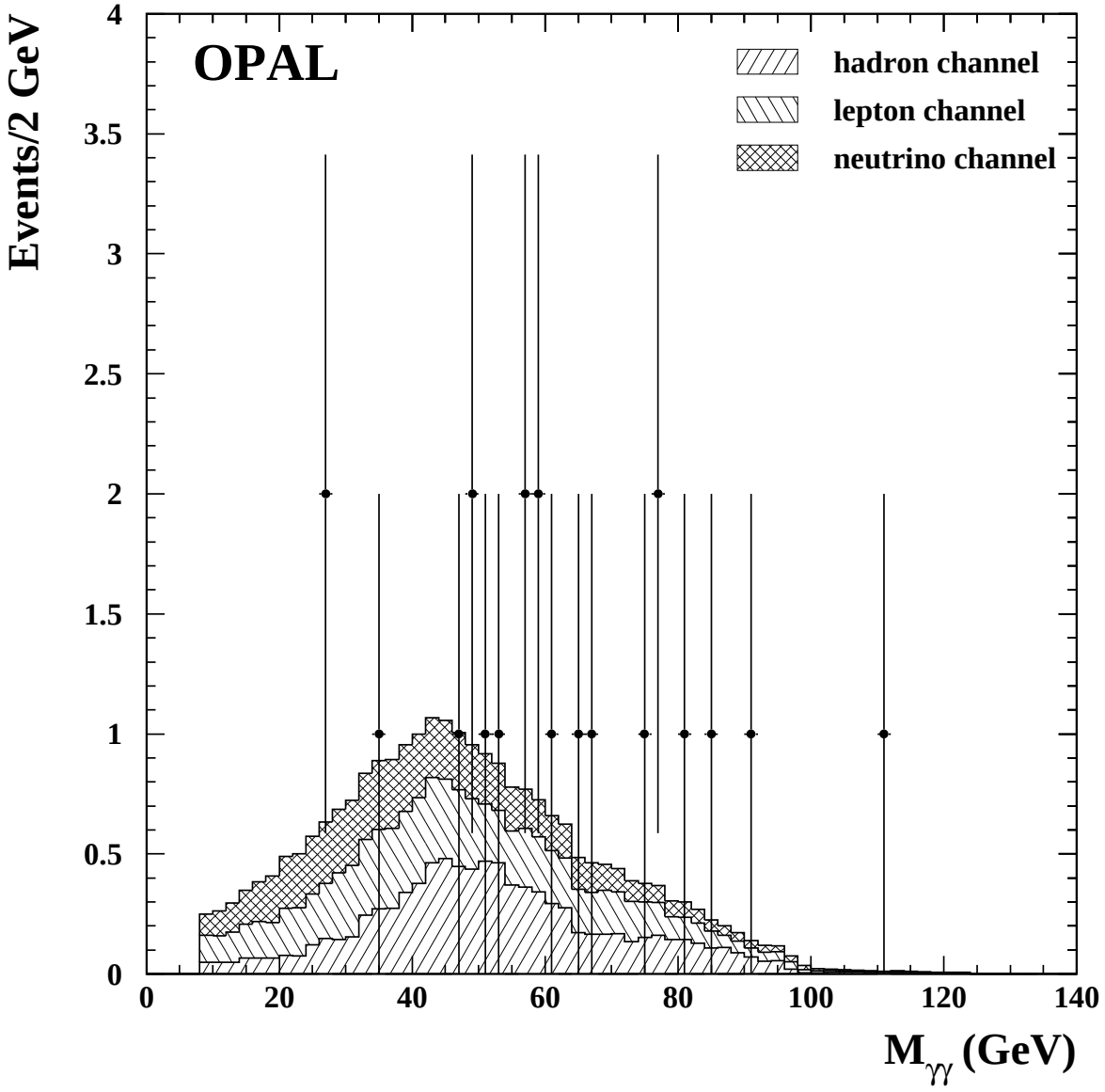

Figure 3: Distribution of mass of the two highest-energy photons in the h^0Z^0 search after application of all selection criteria. All search channels are included. Data are shown as points with error bars. Background simulation is shown as a histogram showing the contributions from the hadronic, charged lepton and missing energy channels as denoted.

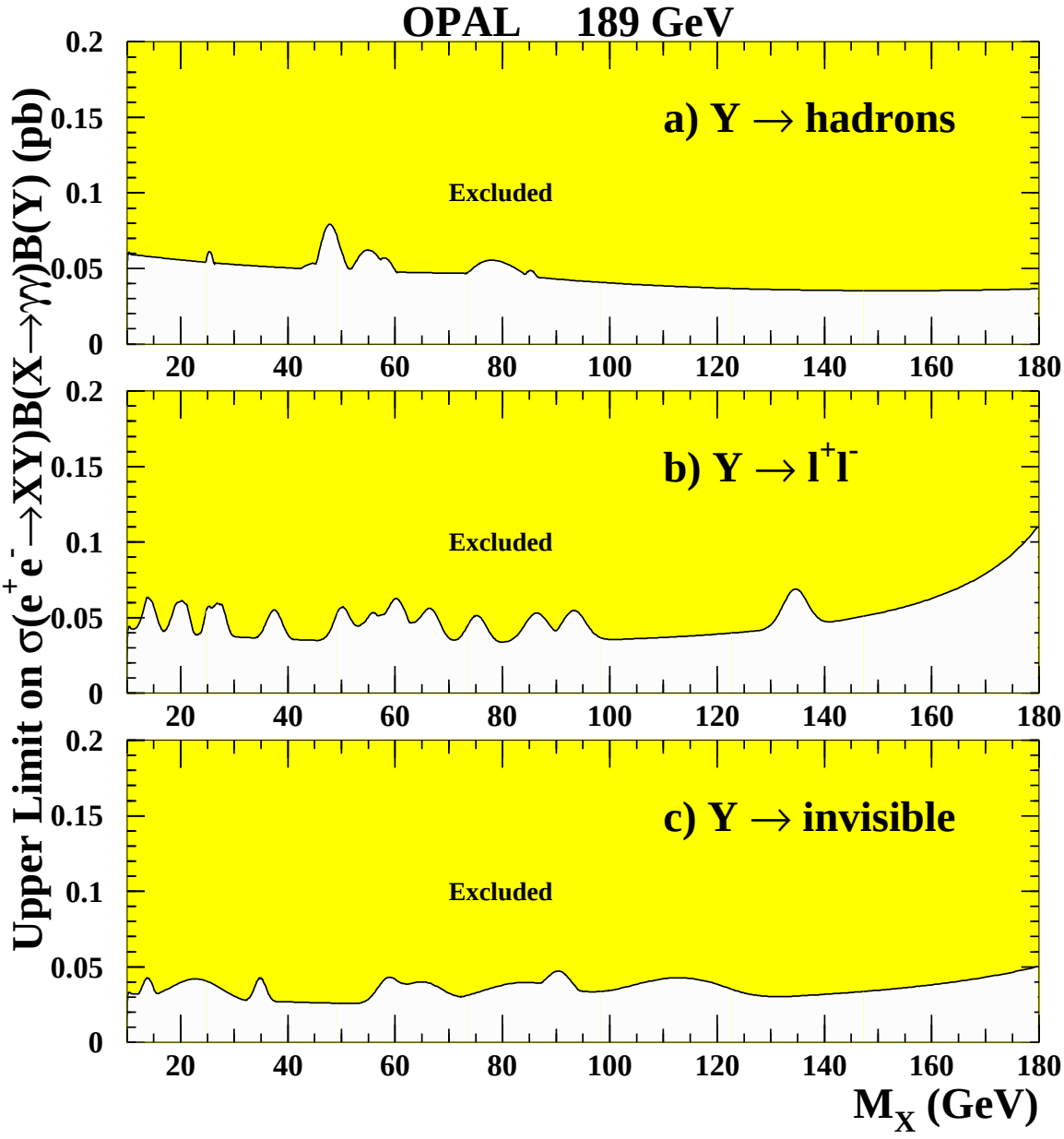

Figure 4: 95% confidence level upper limit on $\sigma(\mathrm{e^+e^-} \to \mathrm{XY}) \times B(\mathrm{X} \to \gamma\gamma) \times \mathrm{B(Y)}$ for the case where: a) Y decays hadronically, b) Y decays into any charged lepton pair and c) Y decays invisibly. The limits for each M_X assume the smallest efficiency as a function of M_Y such that $10 < M_\mathrm{Y} < 180$ GeV and that $M_\mathrm{X} + M_\mathrm{Y} > M_\mathrm{Z}$.

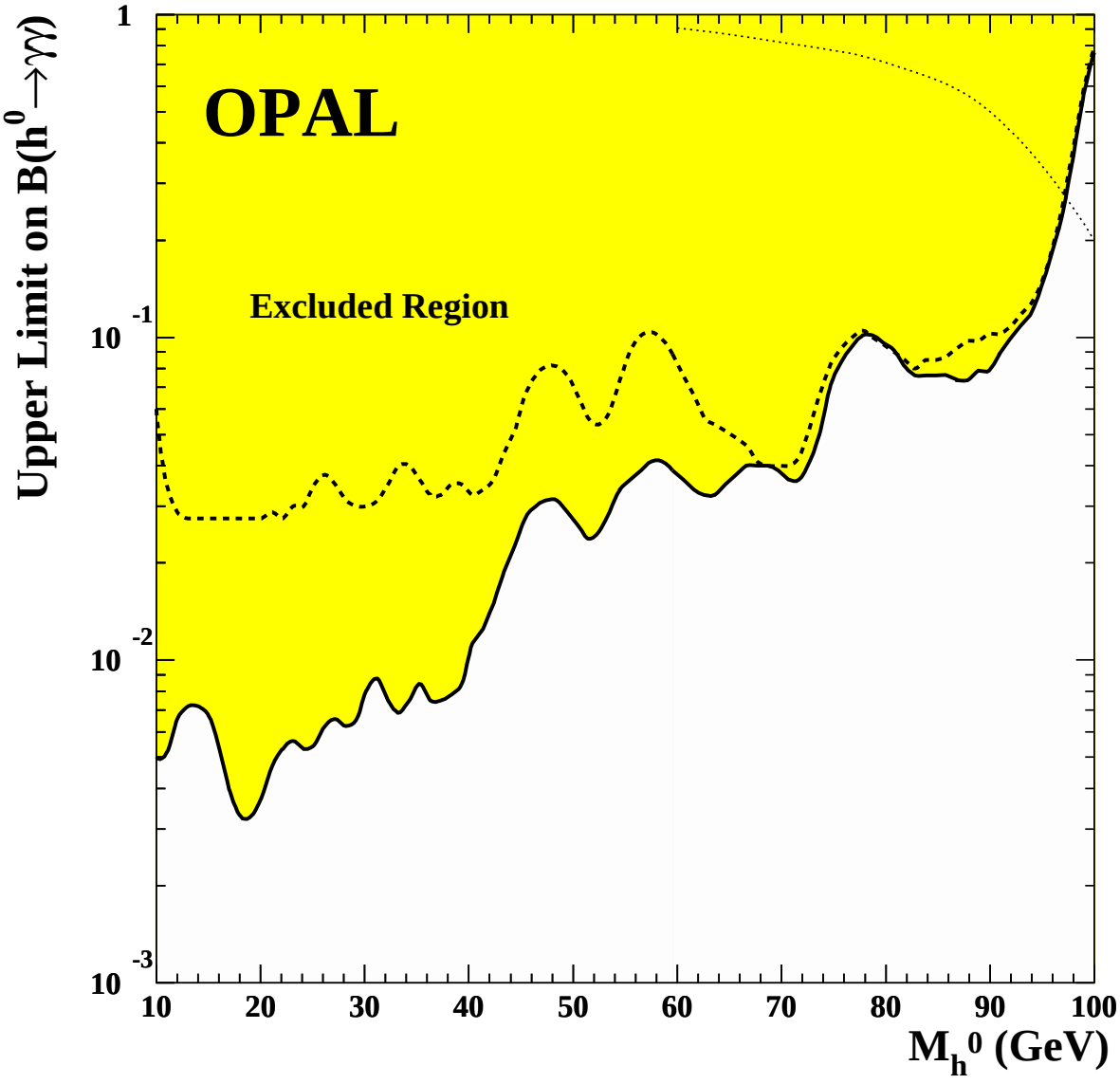

Figure 5: 95% confidence level upper limit on the branching fraction $B(\mathrm{h}^0 \to \gamma\gamma)$ for a Standard Model Higgs boson production rate. The shaded region, obtained with all LEP energies, is excluded; the dashed line shows the limit obtained with the 189 GeV data only. The dotted line is the predicted $B(\mathrm{h}^0 \to \gamma\gamma)$ assuming $B(\mathrm{h}^0 \to \mathrm{f\bar{f}})$=0. The intersection of the dotted line with the exclusion curve gives a lower limit of 96.2 GeV for the fermiophobic Higgs model.